

Progranulin A-mediated MET Signaling Is Essential for Liver Morphogenesis in Zebrafish^{*[S]}

Received for publication, April 30, 2010, and in revised form, September 30, 2010. Published, JBC Papers in Press, October 20, 2010, DOI 10.1074/jbc.M110.138743

Yen-Hsing Li^{†§¶}, Mark Hung-Chih Chen^{||}, Hong-Yi Gong^{**}, Shao-Yang Hu^{††}, Ya-Wen Li[§], Gen-Hwa Lin[§], Ching-Chun Lin[§], Wangta Liu[§], and Jen-Leih Wu^{†§¶1}

From the [†]Molecular and Biological Agricultural Sciences Program, Taiwan International Graduate Program, National Chung Hsing University and Academia Sinica, Taipei 115, Taiwan, the [§]Institute of Cellular and Organismic Biology, Academia Sinica, Taipei 115, Taiwan, the ^{||}Graduate Institute of Biochemistry and Department of Life Sciences, National Chung Hsing University, Taichung 402, Taiwan, the ^{||}Bioluminescence in Life-image Laboratory, Department of Biotechnology, Research Institute of Biotechnology, Hungkuang University, Taichung 433, Taiwan, ^{**}Department of Aquaculture, College of Life Sciences, National Taiwan Ocean University, Keelung 202, Taiwan, and the ^{††}Department of Life Science, National Pingtung University of Science and Technology, Pingtung 912, Taiwan

The mechanism that regulates embryonic liver morphogenesis remains elusive. Progranulin (PGRN) is postulated to play a critical role in regulating pathological liver growth. Nevertheless, the exact regulatory mechanism of PGRN in relation to its functional role in embryonic liver development remains to be elucidated. In our study, the knockdown of progranulin A (GrnA), an orthologue of mammalian PGRN, using antisense morpholinos resulted in impaired liver morphogenesis in zebrafish (*Danio rerio*). The vital role of GrnA in hepatic outgrowth and not in liver bud formation was further confirmed using whole-mount *in situ* hybridization markers. In addition, a GrnA deficiency was also found to be associated with the deregulation of MET-related genes in the neonatal liver using a microarray analysis. In contrast, the decrease in liver size that was observed in *grnA* morphants was avoided when ectopic MET expression was produced by co-injecting *met* mRNA and *grnA* morpholinos. This phenomenon suggests that GrnA might play a role in liver growth regulation via MET signaling. Furthermore, our study has shown that GrnA positively modulates hepatic MET expression both *in vivo* and *in vitro*. Therefore, our data have indicated that GrnA plays a vital role in embryonic liver morphogenesis in zebrafish. As a result, a novel link between PGRN and MET signaling is proposed.

The liver is the largest essential internal organ and has a number of vital functions in the body. The liver parenchyma is largely constituted of hepatocytes (~80%), and the remaining cells include cholangiocytes, Kupffer cells, stellate cells, and sinusoidal endothelial cells (1). Liver organogenesis is initiated in the endodermal cells of the ventral foregut, which develop competence from the cardiac mesoderm to form hepatoblasts. During the specification stages, the specified

hepatoblasts form a liver bud and undergo the hepatic outgrowth process. Hepatic outgrowth is characterized by a large change in the liver bud size that is caused by the rapid proliferation of hepatoblasts. Finally, the hepatoblasts differentiate into functional hepatocytes and cholangiocytes (2, 3). In studies using chicks and mice, liver organogenesis has been shown to be tightly regulated by growth factors, cytokines, and transcription factors. However, little is known about the genetic requirements of the liver growth process and its regulatory mechanism. The use of knock-out mice has led to the discovery of several genes that are critical for hepatic outgrowth. An example of these critical genes is the *met* gene that encodes the hepatocyte growth factor receptor that regulates cell migration, proliferation, morphogenesis, and angiogenesis (4). A knock-out of the *met* gene in mice results in early embryonic lethality and a reduced liver size *in utero* (5). In addition, growth hormone has been shown to be a liver growth-promoting factor (6). To investigate novel regulatory factors involved in liver growth, a subtractive hybridization in conjunction with growth hormone administration was performed. This hybridization led to the identification of progranulin (PGRN)² as a novel growth hormone-regulated growth factor in the liver (7).

PGRN, also known as epithelin/granulin precursor, acrogranin, proepithelin, and PC cell-derived growth factor, is a pleiotropic autocrine growth factor that contributes to early embryogenesis, the wound healing response, frontotemporal dementia, and tumorigenesis (8, 9). PGRN is an extracellular glycoprotein that consists of multiple copies of the cysteine-rich granulin motif. Elevated PGRN levels often occur in patients with cancer, and epidemiological studies show that PGRN is overexpressed in 70% of hepatocellular carcinoma (HCC) patients. Overexpression of PGRN promotes the growth and invasion of HCC cells (10). Treatment with a PGRN monoclonal antibody has been shown to block the established HCC tumor growth in a mouse xenotransplantation

* This work was supported by National Science Council 97-2317-B-001-002 Grant (to J.-L. W.) and National Science Council 97-2313-B-241-001-MY3 Grant (to M. H.-C. C. and J.-L. W.) from the National Science Council of Taiwan.

[S] The on-line version of this article (available at <http://www.jbc.org>) contains supplemental Table S1 and Fig. S1.

¹ To whom correspondence should be addressed: ICOB, No. 128, Sec. 2, Academia Sinica, Taipei 11529, Taiwan. Fax: 886-2-27899534; E-mail: jlwu@gate.sinica.edu.tw.

² The abbreviations used are: PGRN, progranulin; HCC, hepatocellular carcinoma; hpf, hours post-fertilization; MO, morpholino; WISH, whole-mount *in situ* hybridization; PH3, phosphohistone H3; PCNA, proliferating cell nuclear antigen; dpf, days post-fertilization; EGFP, enhanced green fluorescent protein.

PGRN Regulates Embryonic Liver Growth

model (11), which suggests that PGRN is involved in regulating pathological hepatocyte growth. Although the dysregulation of embryonic hepatogenesis signaling has been shown to be associated with hepatocarcinogenesis (12), the physiological role of PGRN in hepatogenesis remains unclear.

Zebrafish are an ideal model for studying the physiological role of PGRN in hepatogenesis because early stages of liver organogenesis in zebrafish are similar to those observed in mice (13). There are four PGRN genes (*grnA*, *grnB*, *grnI*, and *grn2*) in the zebrafish genome, whereas only one gene encodes PGRN in mammals. According to the syntenic conservation of chromosomal localization, *grnA* is the orthologue of the mammalian PGRN gene. In zebrafish, the expression of *grnA* has been observed in the anterior endoderm and the liver primordium from 24 to 120 h post-fertilization (hpf) (14), which suggests that *grnA* might contribute to liver development. In the present study, we knocked down GrnA expression using morpholinos (MOs), which resulted in a small liver phenotype in zebrafish. According to the whole-mount *in situ* hybridization (WISH) analysis, we determined that the morphological defect was caused by an impaired hepatic outgrowth. Furthermore, a microarray approach combined with *in vitro* and *in vivo* examinations revealed that GrnA was an upstream factor of MET signaling in liver growth. Taken together, our findings indicate that GrnA is essential for embryonic liver morphogenesis. In addition, our findings also indicate a possible relationship between PGRN and MET signaling.

EXPERIMENTAL PROCEDURES

Fish Strains—The wild-type (AB) zebrafish (*D. rerio*) and the transgenic line Tg(*fabp10*:EGFP) were maintained under standard conditions. The embryos were collected using natural mating and were cultured at 28.5 °C in Ringer's solution (15).

Western Blots and Antibodies—After the embryos were injected with 0.25 ng MOs and ZFL cells (ATCC, CRL2643), they were treated with either 10 μ M MOs or 100 ng/ml human recombinant progranulin (AXXORA, LLC). Next, the protein samples were isolated, and Western blotting was performed as described previously (16). The lysates were hybridized with the following primary antibodies: β -catenin (1:1000, C-18; Santa Cruz Biotechnology), Erk1/2 (1:1000; Santa Cruz Biotechnologies), phospho-Erk1/2 (1:1000, catalog no. 9101; Cell Signaling), Met (1:1000, sc-10; Santa Cruz Biotechnology), human progranulin (PG359-7; AXXORA, LLC), and actin (1:7500, MAB1501R; Millipore). The polyclonal anti-GrnA antibody was produced using the 4 multiple antigen peptide EWED-HKQKKPETQRTTTRPTG (corresponding to residues 244–264 of GrnA) to immunize BALB/c mice (LTK Biolab, Inc.).

Quantitative RT-PCR—The expression levels of the genes involved in MET signaling were assessed in embryos treated with either MOs or with MOs co-injected with *grnA* mRNA at 72 hpf. First-strand cDNAs were synthesized using the Superscript III first-strand synthesis system (Invitrogen), and primers were designed using Primer Express software (version 2.0, Applied Biosystems). Quantitative RT-PCR analysis was performed using Power SYBR Green PCR Master Mix (Applied Biosystems) as described previously (17). The levels of *ef1a* mRNA were used to normalize the relative mRNA abundance.

Morpholino Knockdown and mRNA Rescue Assay—The *grnA* antisense MO1 (5'-TTGAGCAGGTGGATTTGTGAA-CAGC-3'), MO2 (5'-GGAAAGTAAATGATCAGTCCGT-GGA-3'), and MO1 with five base pair mismatches (5'-TTCAGGAGGTAGATTTGTCAAGAGC-3') (Gene Tools) were administered either by microinjection or delivered into cells via Endo-Porter (Gene Tools) (18) at the designated concentrations. Zebrafish *grnA* (0.25 ng/embryo), *met* (0.25 ng/embryo), and *lacZ* (0.25 ng/embryo) mRNAs were synthesized using the mMACHINE kit (Ambion) and co-injected with *grnA* MOs (0.25 ng/embryo) or *met* MO (CM2, 0.5 ng/embryo) (19) at the one-cell stage of the rescue assay.

Immunohistochemistry, Cell Number Determination, and Whole-mount *in situ* Hybridization—For immunohistochemistry, fixed and paraffin-embedded embryos were sectioned and hybridized with a proliferating cell nuclear antigen (PCNA) antibody (PC10; Abcam) as described previously (20). For whole-mount phosphohistone H3 (PH3) staining, PH3-positive cells were detected using the polyclonal anti-PH3 antibody (Santa Cruz Biotechnology) as the first antibody (1:200). Alexa Fluor 555 goat anti-rabbit IgG antibody conjugated to red fluorescent protein was used as the second antibody (Invitrogen) (1:750) as described previously (21). Hematoxylin and eosin staining were used to determine the size of hepatocyte. Sections and confocal images that were acquired using a Leica SP5 confocal microscope were analyzed using MetaMorph software (version 6.1). Control and *grnA* MO-injected Tg(*fabp10*:EGFP) embryos were trypsinized and homogenized to calculate the percentages of GFP-expressing liver cells among the total cells by flow cytometry. For WISH, antisense digoxigenin probes for *cp* (GenBankTM accession no. NM_131802), *cebpb* (GenBankTM accession no. NM_131884), *dlx3b* (GenBankTM accession no. NM_131322), *fabp10* (GenBankTM accession no. NM_152960), *hand2* (GenBankTM accession no. NM_131626), *myod* (GenBankTM accession no. NM_131262), and *sePb* (GenBankTM accession no. XM_001923882) were generated by *in vitro* transcription using T7 or SP6 RNA polymerase as described previously (22).

BrdU Incorporation and TUNEL Assays—For BrdU *in vivo* labeling, 4-dpf embryos were incubated for 4 h at 28.5 °C in a 5-bromo-2-deoxyuridine (BrdU) solution (10 mM; Roche Applied Science) and were fixed in 4% PFA for 24 h before being used for immunohistochemistry as described previously (21). For the TUNEL assay, 4-dpf embryos were fixed in 4% PFA overnight, washed for 30 min in PBS, and incubated in a permeabilization solution (0.1% Triton X-100, 0.1% sodium citrate) for 2 min on ice. Paraffin-embedded sections were used for the *In Situ* Cell Death Detection kit, TMR red (Roche Applied Science).

Microarrays—RNA samples were extracted, and oligo(dT)-primed cDNAs were prepared using the SuperScript III RT kit (Invitrogen). Microarray experiments were performed using the zebrafish 14K oligo microarray (MWG Biotech Ltd.) according to a previously described protocol (23). The data were submitted to NCBI Gene Expression Omnibus (accession no. GSE19211).

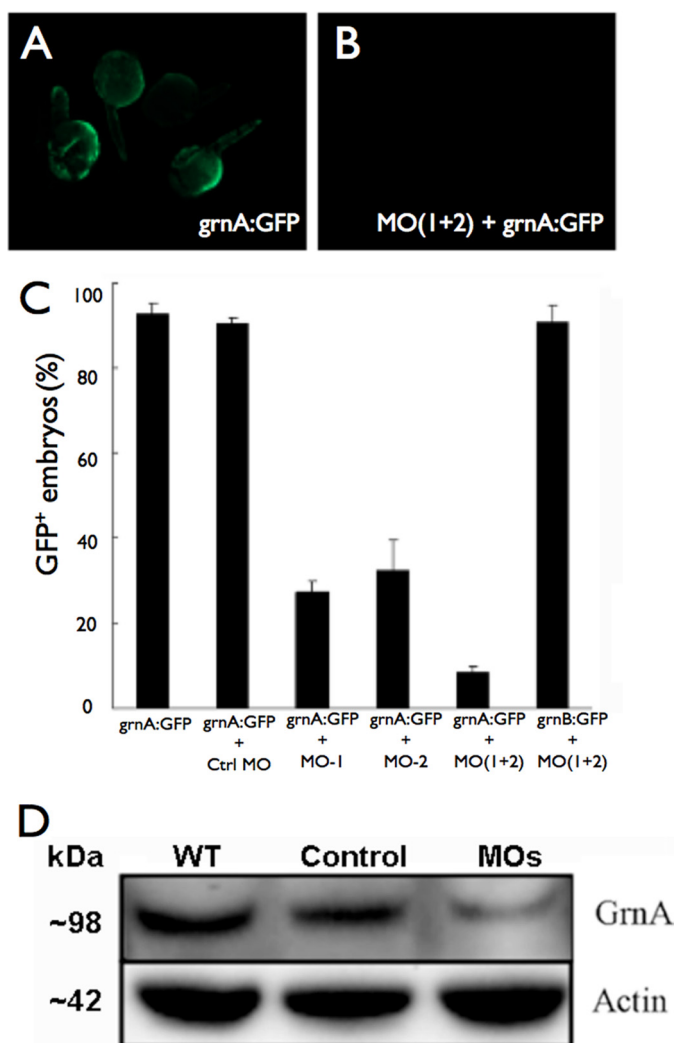


FIGURE 1. Antisense MOs specifically and efficiently knock down GrnA *in vivo*. *A*, microinjection of the *grnA*:GFP validation vector led mosaic GFP expression at 24 hpf. *B*, compared with injection of the *grnA*:GFP vector alone, co-injection of *grnA*:GFP with MOs decreased GFP expression. *C*, the administration of a mixture of MO1 and MO2 showed the strongest inhibition of GFP expression, whereas the expression of *grnB*:GFP was not affected by the MO treatments. *D*, the expression levels of GrnA in whole embryos were significantly suppressed on day 4 after MO administration. Actin expression was evaluated as a loading control. Error bars indicate S.D.

RESULTS

Antisense MOs Specifically and Efficiently Knock Down GrnA—To study the genetic requirement of GrnA in embryonic liver development, we designed two *grnA*-specific MOs for GrnA knockdown, MO1 and MO2, which targeted two adjacent sequences in the 5'-untranslated region of the *grnA* coding sequence. A version of MO1 that contained five mismatched mutations was used for the control injections. The MO knockdown efficiencies were examined by assessing the CMV promoter-driven expression of the GFP-tagged *grnA* targeting sequence (*grnA*:GFP) or the *grnB* targeting sequence (*grnB*:GFP) following MO injection. An increase in mosaic GFP expression was observed after microinjection of the *grnA*:GFP plasmid (100 pg/embryo) into zebrafish embryos (Fig. 1*A*). A co-injection of *grnA*:GFP with either of the antisense MOs (0.25 ng) decreased GFP fluorescence in the em-

bryos at 24 hpf (Fig. 1*B*); however, a control MO injection failed to block the GFP expression (Fig. 1*C*). A co-administration of the *grnA*:GFP vector with a 0.25-ng mixture of MO1 and MO2 (MOs) led to a much stronger inhibition of GFP expression compared with either antisense MO alone. In addition, the expression of *grnB*:GFP was not inhibited by MOs (Fig. 1*C*), which suggested that the *grnA* MO had a high specificity and no off-target effects. Because administration of the 0.25 ng mixture of MOs caused the greatest GFP suppression, we used this treatment for the subsequent experiments. Next, we measured the expression of the GrnA protein following MO treatment by Western blotting. We found that the expression of GrnA was suppressed by MO treatment at 4 dpf compared with the wild-type mice and the control MO treatments (Fig. 1*D*). These results demonstrated that the MOs specifically and efficiently knocked down GrnA expression.

Knockdown of GrnA Confers a Small Liver Phenotype—To study the role of *grnA* in liver development, 0.25 ng of MOs were injected into Tg(*fabp10*:EGFP) zebrafish. This procedure has been shown to result in the liver-specific expression of enhanced green fluorescent protein (EGFP) from 36 hpf (24). The control and mock-injected Tg(*fabp10*:EGFP) zebrafish embryos expressed intact EGFP in the liver at 4 dpf, whereas the *grnA* morphants exhibited a significant decrease in EGFP expression (Fig. 2*A*, 69.3%, $n = 300$). A histological analysis was performed to assess the hepatocyte size in *grnA* morphants. The cell size was determined by measuring the area of a single hepatocyte using MetaMorph software (version 6.1). The MO administration decreased the mean hepatocyte area compared with that measured in controls ($810.6 \pm 160 \mu\text{m}^2$ in controls versus 480 ± 133 in *grnA* morphants based on 10 randomly selected hepatocytes at 4 dpf; $n = 3$; Fig. 2, *B* and *D*). The smaller liver size was quantified by measuring the fluorescence intensity in three-dimensional confocal images. At 4 dpf, the liver volume in the control MO-injected Tg(*fabp10*:EGFP) embryos was $6.8 \pm 0.2 \times 10^{-3} \text{ mm}^3$ ($n = 30$), and the liver size in the *grnA* morphants was reduced to 22% of that determined in the controls ($1.5 \pm 0.3 \times 10^{-3} \text{ mm}^3$, $n = 30$, Table 1). To further characterize the smaller liver according to the number of cells, we examined the ratio of the GFP-expressing liver cells to the cell numbers present in the whole embryo via flow cytometry. This liver-over-body ratio in the *grnA* morphants was 0.37 times that determined in the control group (3.8 ± 0.7 in the control group versus 1.4 ± 0.6 in *grnA* morphants based on 20 embryos at 4 dpf; $n = 3$, Table 1). These findings demonstrate that *grnA* morphants have a small liver phenotype.

GrnA Is Crucial for Liver Morphogenesis—Established markers were applied to understand the developmental defects caused by GrnA knockdown. To examine the endoderm-derived tissue in the *grnA* morphants, insulin, a marker of islet, revealed a similar pattern in the controls and the *grnA* morphants at 72 hpf (Fig. 3, *A–B*, 93%, $n = 30$). The expression pattern of trypsin (an exocrine pancreas marker) was also similar in the controls and the *grnA* morphants; however, a slightly reduced size was observed in the GrnA knockdown embryos (Fig. 3, *C–D*, 83%, $n = 30$). We further examined liver development using the panendodermal markers fork-

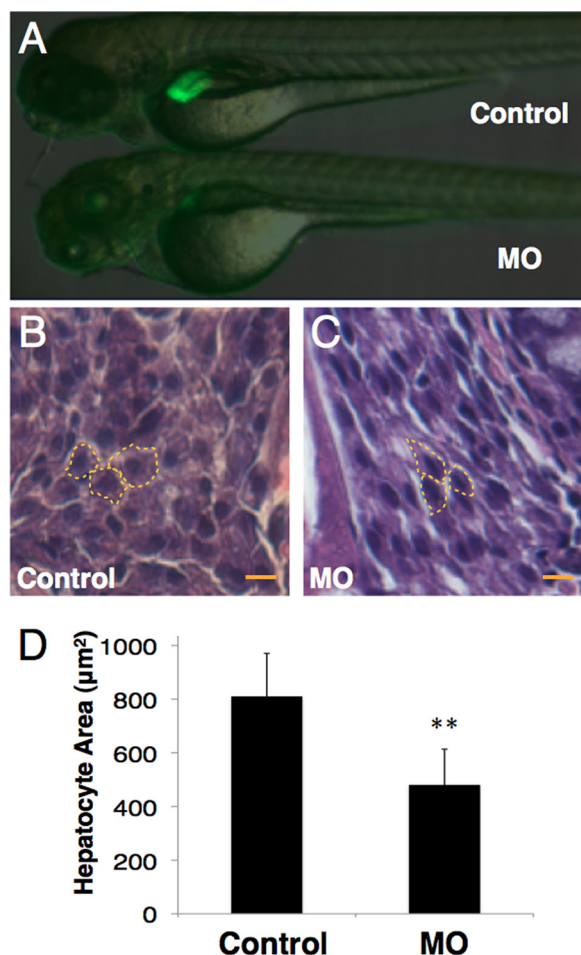


FIGURE 2. Liver morphology of 4-dpf *grnA* morphants. *A*, liver morphology at 4 dpf. Compared with fish that were injected with a MO containing mutations in five base pairs, the EGFP expression of Tg(*fabp10*:EGFP) zebrafish faded after MO (0.25 ng/embryo) administration. *B* and *C*, hematoxylin and eosin stained hepatocyte sections from *grnA* morphants. The cell size was determined by measuring the area of a single hepatocyte (dotted line). MO administration decreased the mean hepatocyte area as compared with the controls ($n = 3$). Scale bars, 25 µm. **, $p < 0.01$, *t* test. Error bars indicate S.D.

TABLE 1

Morphant phenotype characterization at 4 days post-fertilization

Data are presented as the means ± S.E.

	Liver volume	Body length	Liver/body ^a
	10 ⁻³ mm ³	mm	%
Control	6.8 ± 0.2	4.1 ± 0.1	3.8 ± 0.7
MO	1.5 ± 0.3	4.0 ± 0.2	1.4 ± 0.6

^a The ratio of GFP-expressing cells to the whole body cell number is shown.

head box A3 (*foxA3*) and CCAAT/enhancer binding protein beta (*cebpb*), which are expressed in endodermal digestive organs. Interestingly, the liver size was reduced in the *grnA* morphants at 72 and 96 hpf, whereas the intestine and pancreas were less affected (Fig. 3, *E* and *F*, 76%, $n = 25$; Fig. 3, *G* and *H*, 70%, $n = 30$, respectively). Without causing a widespread developmental defect, using the intestinal marker fatty acid binding protein 2 (*fabp2*), we discovered similar intestinal patterns in the controls and MO-treated embryos at 72 hpf (Fig. 3, *O* and *P*, 90%, $n = 30$). In addition, the expression pattern of the ectoderm marker distal-less homeobox gene 3b (*dlx3b*) was indistinguishable between the controls and *grnA*

knockdown embryos at 8 hpf (Fig. 3, *I* and *J*, $n = 20$). Two mesodermal genes, heart and neural crest derivatives expressed transcript 2 (*hand2*) and myogenic differentiation 1 (*myod*), displayed similar expression levels in *grnA* morphants at 30 and 54 hpf, respectively (Fig. 3, *K–L*, $n = 25$; Fig. 3, *M* and *N*, $n = 25$). Our results demonstrate that GrnA plays a crucial role in liver morphogenesis.

GrnA Is Required for Hepatic Outgrowth but Not for Hepatoblast Specification—To determine the stages that were affected by *grnA* knockdown during liver morphogenesis, we examined liver developmental markers in *grnA* morphants. Using the specification markers hematopoietically expressed homeobox (*hhex*) and prospero-related homeobox 1 (*prox1*), which are expressed in definitive hepatoblasts (25), the knockdown of GrnA resulted in a normal expression pattern of both *hhex* and *prox1* at 24 hpf (Fig. 4*B*, 85%, $n = 20$ and Fig. 4*E*, 75%, $n = 20$). However, at the later stage, when the liver size had increased moderately, reduced levels of *hhex* and *prox1* expression were observed in the *grnA* morphants at 72 hpf (Fig. 4*H*, 68%, $n = 25$ and Fig. 4*K*, 57%, $n = 30$). The decrease in liver size was restored using a co-injection of *grnA* mRNA (0.25 ng/embryo) with MOs (Fig. 4*I*, 88%, $n = 25$ and Fig. 4*L*, 80%, $n = 30$). Furthermore, we applied the fatty acid binding protein 10 (*fabp10*) marker to examine liver function; *fabp10* expression was markedly decreased in 72-hpf *grnA* morphants (Fig. 4*N*, 83%, $n = 30$), which suggests an impaired hepatocyte maturation in these *grnA* morphants. Additionally, the decrease of *fabp10* expression was largely recovered in the *grnA* mRNA rescue experiment (Fig. 4*O*, 76%, $n = 100$). In conclusion, our results indicate that the knockdown of GrnA suppresses hepatic outgrowth and maturation but not liver specification.

Knockdown of GrnA Impairs Liver Cell Proliferation and Enhances Apoptosis—We performed whole-mount immunohistochemistry to examine the terminal fate of the GrnA-deficient hepatocytes. Using an antibody against PH3, a marker of cell proliferation, the PH3-positive hepatocytes exhibited a 6.5-fold reduction in the 4-dpf *grnA* morphants (Fig. 5, *A* and *B*, 10.4 cells in the controls versus 1.6 in the *grnA* morphants based on three sections per embryo; $n = 5$), whereas in the same sections, only a 3.3-fold decrease was observed in the number of PH3-positive cells in the peripheral tissues (Fig. 5, *A* and *B*, 32.8 cells in the controls versus 9.9 in the *grnA* morphants based on three sections per embryo; $n = 5$). Furthermore, an analysis using the antibody against PCNA and BrdU demonstrated similar results. The number of PCNA-positive hepatocytes was decreased in the *grnA* knockdown morphants compared with the control embryos at 4 dpf, as measured by the mean number of PCNA-stained cells (supplemental Fig. S1, *A–C*, 36.2 cells in the controls versus 19.6 in the *grnA* morphants based on three sections per embryo; $n = 3$). BrdU is specifically incorporated into DNA during S-phase. The liver fraction of BrdU-labeled cells in the *grnA* morphants was greatly reduced compared with the controls (Fig. 5, *B* and *C*, $n = 5$). Next, we examined the apoptotic events after GrnA knockdown using the TUNEL assay. Compared with the controls, DNA strand breaks that occur during apoptosis were detected in the livers of the *grnA* morphants at

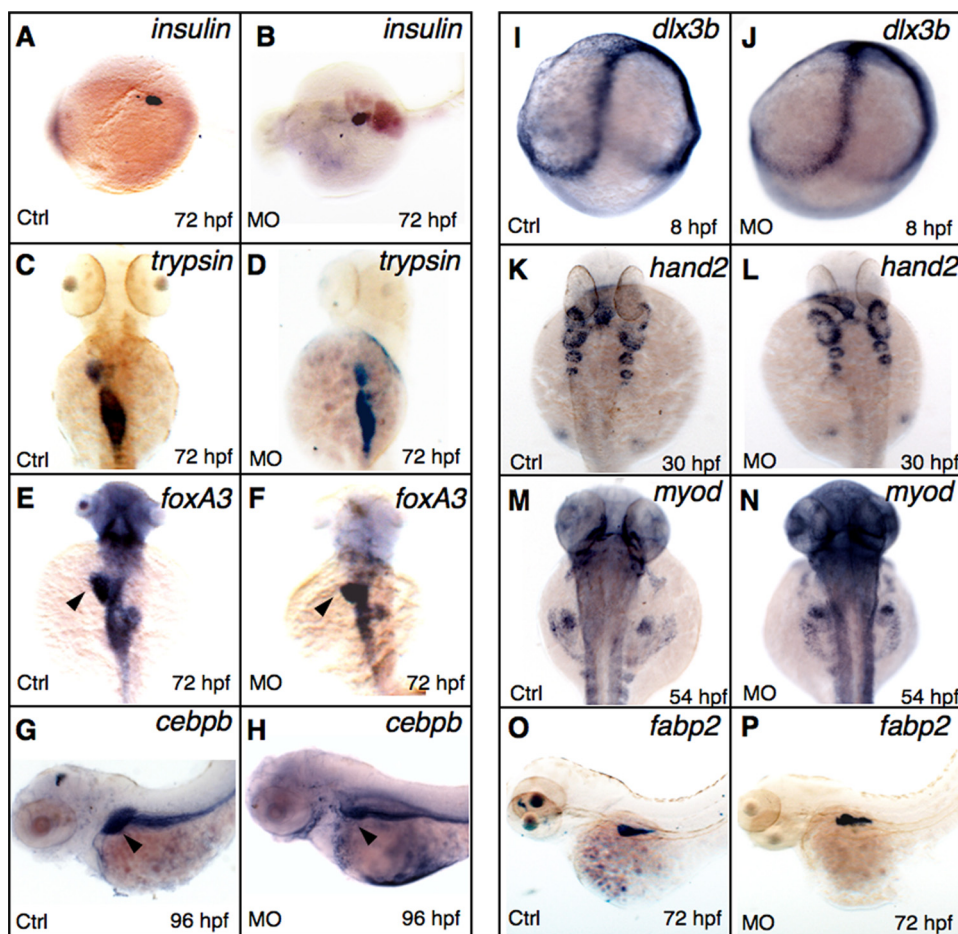


FIGURE 3. Whole-mount *in situ* hybridization of *GrnA* knockdown embryos. Expression patterns of the marker genes insulin (A and B), trypsin (C and D), *fabp2* (O and P), and *foxA3* at 72 hpf (E–H), *dlx3b* at 8 hpf (I and J), *myod* at 54 hpf, and *hand2* at 30 hpf (K–N), were examined using WISH in the controls (Ctrl) and *grnA* morphants. C–F and K–N, dorsal views, anterior up; A, B, G, H, O, and P, lateral views, anterior left.

4 dpf (Fig. 5, E and F, $n = 5$). Consequently, the *GrnA*-deficient hepatocytes were impaired with respect to their proliferation abilities and showed an increased frequency of programmed cell death.

***MET* Is Involved in *GrnA*-regulated Liver Growth**—To explore the changes in *GrnA* knockdown-induced gene expression during liver outgrowth, the mRNA expression profiles of the controls and *grnA* MO-injected embryos were compared at 72 hpf using a zebrafish 14K oligonucleotide microarray. According to the gene set enrichment analysis, the differentially expressed genes were found to be associated with cell cycle regulation, DNA replication, ubiquitin-dependent protein degradation, apoptosis regulation, transcription and translation control, chromatin remodeling, and focal adhesion regulation (supplemental Table S1). To determine the major regulatory signaling pathway that was affected by *grnA* knockdown, the microarray data were processed using Pathway Studio analysis software (version 7.0). The results indicated that a number of *MET* expression-related genes, including *mmp2* (26), *mif* (27), *ybx1* (28), *ctnbn1* (29), *sub1* (30), *rac1* (31), *rps6kb1* (32), *fn1* (33), and *cdh2* (34), were down-regulated in the context of *GrnA* deficiency. *MET*, which encodes a receptor tyrosine kinase, is known to be critical for liver size in mice (5) and zebrafish (35). The suppressed expression of

MET-related genes was further confirmed using quantitative RT-PCR in 72-hpf *grnA* morphants (Fig. 6A). We also examined the expression levels of genes that are involved in cell proliferation. The expression levels of *ccna2*, *jnk1*, and the *PCNA* gene were decreased in the 72-hpf *grnA* morphants. Interestingly, the expression levels of TGF β signaling factors (*tgfb1*, *smad3a*, and *smad4*) and hepatocyte growth factors (*hgf1* and *hgf2*) were influenced very little by *GrnA* knockdown (Fig. 6B).

GrnA* Regulates Hepatic Outgrowth via *MET—We conducted mRNA rescue experiments to verify whether *GrnA* regulated hepatic outgrowth via *MET* signaling. A significant reduction in liver size was observed in the 96-hpf *grnA* morphants (Fig. 2A and Fig. 7H, 70%, $n = 300$). In addition to co-injecting *grnA* mRNA (Fig. 7I, 76%, $n = 300$), co-injections *met* mRNA with *grnA* MOs in Tg(*fabp10*:EGFP) embryos restored the normal liver size (Fig. 7J, 51%, $n = 300$). Furthermore, we knocked down *MET* expression by injecting a validated *met* MO (19) that led to an impaired liver size at 4 dpf (Fig. 7K, 40.7%, $n = 300$). However, a co-injection of *grnA* mRNA (0.25 ng/embryo) with *met* MO still led to a small liver size (Fig. 7L, 68%, $n = 300$). Similar results were obtained for the *foxA3* expression at 50 hpf. The co-injection of *met* mRNA with *grnA* MO restored the loss of *foxA3* expression in

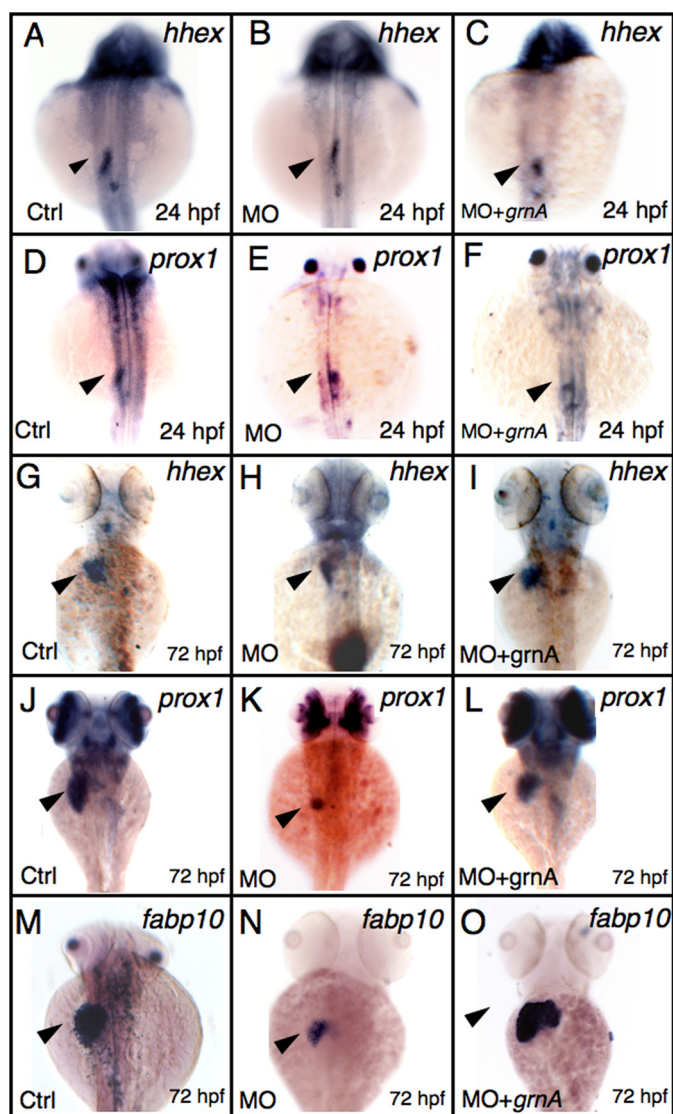


FIGURE 4. Knockdown of GrnA blocks hepatic outgrowth but not specification. The expression levels of *hhx* (A–C) and *prox1* (D–F) were examined using WISH in the controls and *grnA* morphants at 24 hpf (dorsal views, anterior up). The controls and *grnA* morphants were examined using WISH with *hhx* and *prox1* (G–I and J–L) and *fabp10* (M–O; maturation marker) at 72 hpf (dorsal views, anterior up). Co-injection of *grnA* mRNA (0.25 ng/embryo) and MO into one-cell embryos restored the deficient expression of the marker genes (I, L, and O). The arrowhead indicates the developing liver (A–C). Ctrl, control.

the *grnA* morphants (Fig. 7D, 60%, $n = 20$). In contrast, a co-injection of *grnA* mRNA with *met* MO did not compensate for the impaired *foxA3* expression in the *met* morphants (Fig. 7F, 80%, $n = 20$).

GrnA Positively Modulates Hepatic *met* Expression—To examine the regulation between GrnA and MET signaling in liver cells, we applied *grnA* MOs (10 μ M) in ZFL cells (zebrafish liver cell line) to assess the protein expression of MET signaling following *grnA* knockdown. At 48 h after the administration of MOs, the protein expression levels of GrnA were significantly reduced 0.6-fold compared with those determined in untreated and control MO-treated cells, as shown using Western blotting (Fig. 8A and C, GrnA/actin ratio, $n = 3$). Following *grnA* knockdown, the protein expression of

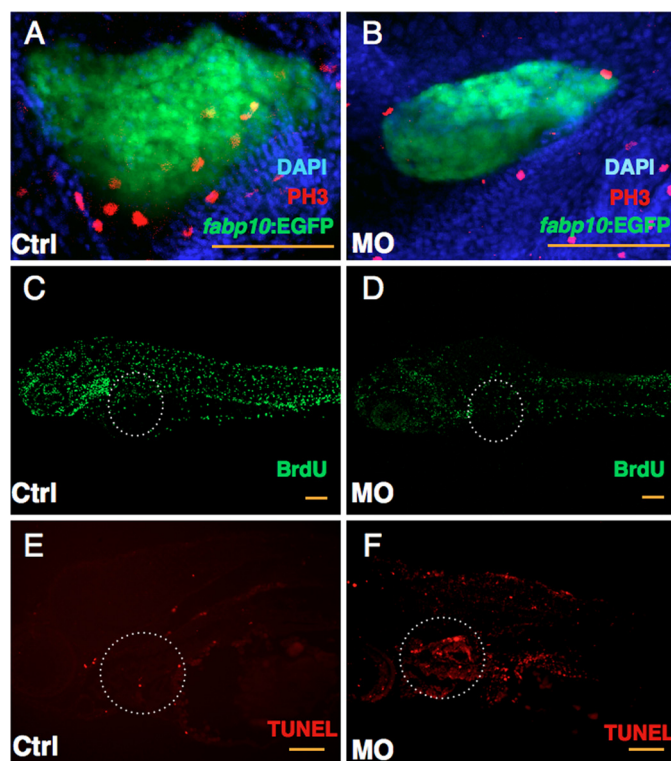


FIGURE 5. Knockdown of GrnA impairs liver cell proliferation and enhances apoptosis. Control (Ctrl) and *grnA* MO-injected embryos were examined using the anti-PH3 antibody, BrdU incorporation, and a TUNEL assay at 4 dpf. DAPI was used to stain the cell nuclei. Fewer PH3-positive cells were detected in MO-injected Tg (*fabp10:EGFP*) embryos compared with control MO-treated embryos at 4 dpf (A and B). BrdU incorporation was suppressed in the liver in *grnA* morphants compared with controls (C and D). TUNEL staining of control MO-injected embryos (E) and knockdown embryos (F). A dotted line circles the liver. Scale bars, 100 μ m.

MET and the downstream phosphorylated ERK1/2 and β -catenin were significantly decreased in MO-treated cells (Fig. 8, A and C, $n = 3$). In contrast, treatment with recombinant human PGRN (100 ng/ml) increased MET, phosphorylated ERK1/2, and β -catenin protein expression at 2 h post-PGRN administration (Fig. 8, B and D, $n = 3$). These results suggest that PGRN positively regulates MET signaling in zebrafish liver cells. In addition to the *in vitro* analyses, we further confirmed this regulation in zebrafish embryos via WISH. We found that *met* expression was decreased in the liver region of the *grnA* morphants (Fig. 8F, 57%, $n = 30$). In addition, the hepatic *met* expression was restored by a co-injection of *grnA* mRNA with MOs at 96 hpf (Fig. 8G, 87%, $n = 30$), which indicates that GrnA positively modulates hepatic *met* expression *in vivo*.

DISCUSSION

The dysregulation of embryonic growth factors, receptors, and their downstream signaling components in adulthood has been shown to promote HCC proliferation and invasiveness (12). Although PGRN has been shown to be involved in HCC progression, the functional role of PGRN in embryonic liver organogenesis remains unknown. In the present study, we addressed two major issues. First, we assessed whether PGRN is involved in embryonic liver development. Second, we investigated the molecular mechanisms of PGRN in the regulation

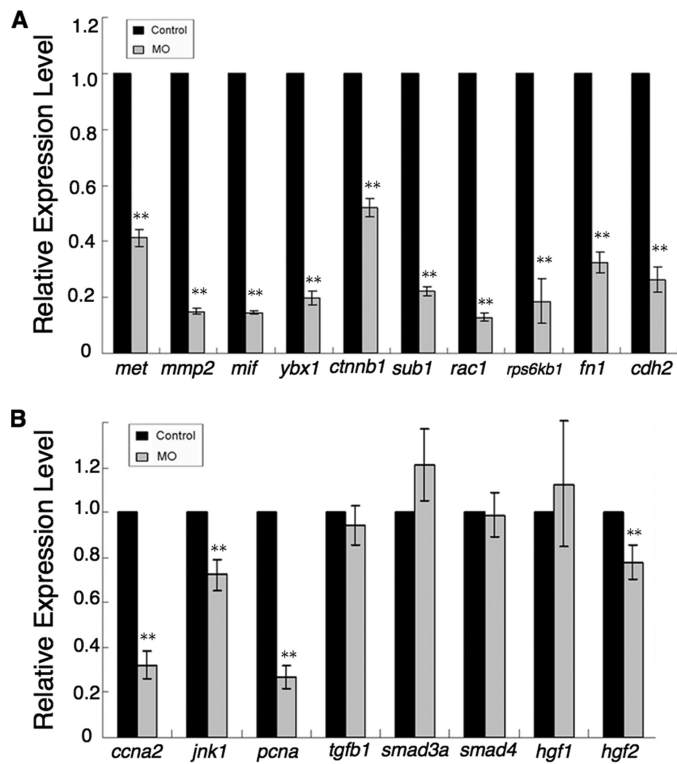


FIGURE 6. GrnA deficiency decreases the expression of MET-related genes. Transcriptional expression levels of MET signaling-related genes (*met*, *mmp2*, *mif*, *ybx1*, *ctnnb1*, *sub1*, *rac1*, *rps6kb1*, *fn1*, and *cdh2*) (A) and other genes involved in liver growth (B) were examined using quantitative RT-PCR in 72-hpf controls and *grnA* morphants. The expression level of *ef1a* served as an internal control. The experiment was performed in triplicate; error bars indicate S.D. **, $p < 0.01$, *t* test.

of liver growth. To study the genetic requirement of PGRN in embryonic liver development, we inhibited PGRN by antisense morpholino knockdown of the PGRN orthologue *grnA* in zebrafish. The Tg(*fabp10*:EGFP) model showed that GrnA knockdown led to a reduced liver size, which was verified using confocal imaging and immunohistochemistry (Fig. 2 and Table 1). This reduction suggests that GrnA is required for liver morphogenesis in zebrafish. An important issue is whether GrnA is specific for liver morphogenesis. PGRN is maternally deposited and then expressed zygotically in a number of epithelial cells, including the skin, the gastrointestinal tract, and immune cells (36). In addition to the liver, our analysis revealed that GrnA affected the development of several tissues, including the pancreas and blood cells (Fig. 3 and data not shown). It is possible that *grnA* is widely expressed in many tissues in the zebrafish embryo (14); therefore, its expression is required for the development of various tissues. However, during embryonic development, the liver is much more sensitive to a GrnA deficiency compared with other endoderm, mesoderm, and ectoderm-derived tissues (Fig. 3). This sensitivity indicates that GrnA plays a crucial role in liver organogenesis. Furthermore, we applied established WISH markers to frame the developmental stages that were affected by *grnA* knockdown and that led to impaired liver morphogenesis. At 24 hpf, the expression of *hhex* and *prox1* led to normal liver bud formation, which suggested that specification was not disrupted in the *grnA* morphants. In contrast,

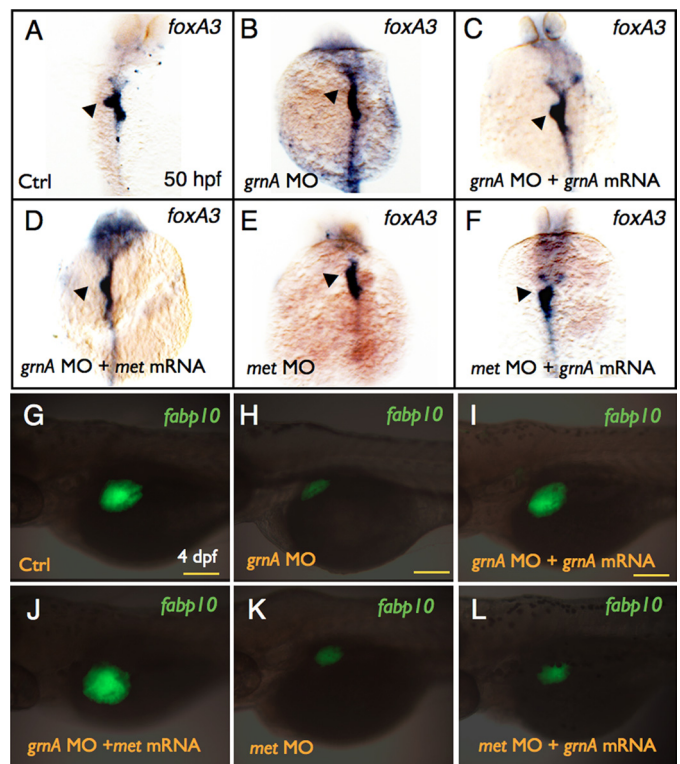


FIGURE 7. Effect of *grnA* and *met* on liver formation. Whole-mount *in situ* hybridization of *foxA3* expression in 50-hpf embryos injected with control MO (A), *grnA* MO (B), *grnA* MO with *grnA* (C) or *met* (D) mRNA, *met* MO (E), and *met* MO with *grnA* mRNA (F). EGFP expression in 4-dpf Tg(*fabp10*:EGFP) embryos that were injected with control MO (G), *grnA* MO (H), *grnA* MO with *grnA* (I) or *met* (J) mRNA, *met* MO (K), and *met* MO with *grnA* mRNA (L) (dorsal views, anterior up). The liver is indicated by the arrowhead. Ctrl, control. Scale bars, 100 μ m.

our WISH results showed that hepatic outgrowth had been attenuated early with respect to the expression of ceruloplasmin from 40 hpf (data not shown) and *foxA3* at 50 hpf (Fig. 7B). The expression of *hhex*, *prox1*, *fabp10*, *foxA3*, and *cebpb* in 72- and 96-hpf *grnA* morphants might have also led to the defective hepatic outgrowth observed in *grnA* morphants. Therefore, we conclude that GrnA is required for hepatic outgrowth rather than for specification in zebrafish. Numerous genes have been identified that are required for outgrowth, and it has been demonstrated that a loss of the expression of these genes decreases hepatic proliferation and leads to apoptosis (37–40). PGRN has been reported to be a growth factor that stimulates cell proliferation (41, 42) and decreases apoptosis (43–45). The present work is the first to show that PGRN is involved in embryonic liver growth regulation. A loss of GrnA expression led to impaired proliferation and enhanced apoptosis in zebrafish embryos (Fig. 5 and supplemental Fig. S1). Similarly, the reduction of PGRN protein has been shown to suppress HCC proliferation in a nude mouse xenotransplantation model (10, 11), which suggests a relevant regulatory mechanism of PGRN in HCC proliferation and embryonic liver growth. Besides, recent reports showed that the PGRN knock-out mice display behavioral abnormalities and dysregulated inflammation and neuropathology (46–48). In contrast to our results shown in 4 dpf *grnA* knockdown zebrafish (Table 1), the ratio of liver weight over whole body

PGRN Regulates Embryonic Liver Growth

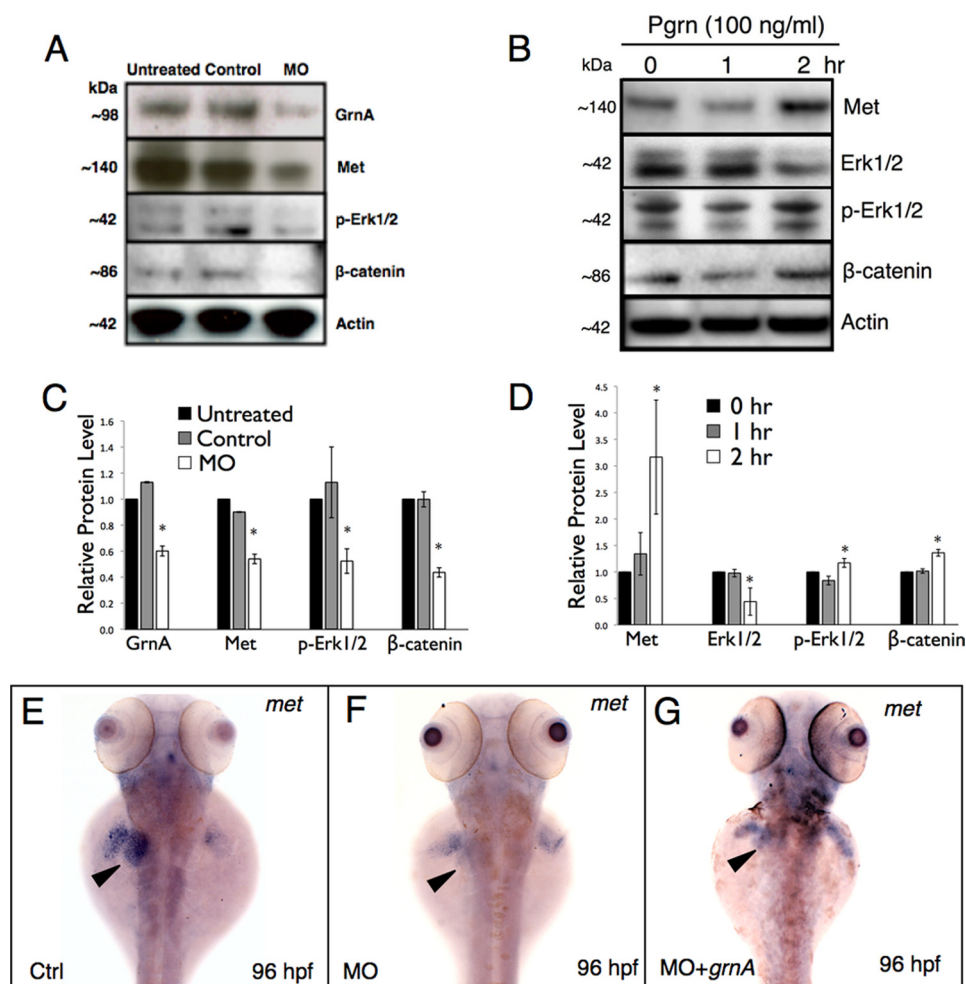


FIGURE 8. GrnA positively modulates hepatic *met* expression *in vitro* and *in vivo*. Protein levels of GrnA, MET, ERK1/2, phosphorylated ERK1/2, β -catenin, and actin were examined by Western blot analysis in ZFL cells at 48 h post-*grnA* knockdown (A) and recombinant human PGRN treatment (B; 100 ng/ml). The relative GrnA, MET, ERK1/2, and β -catenin protein levels in each treatment were quantified as shown in the lower panel (C and D; normalized to the actin level). The expression of *met* in the liver region (E–G; arrowhead) was determined using WISH in controls, *grnA* morphants, and *grnA*-rescued embryos at 96 hpf. Ctrl, control. *, $p < 0.05$, t test. Error bars indicate S.D.

weight is normal in the 2-month-old PGRN knock-out mice (47). However, the detail examination remains to be seen whether the liver development is impaired in these animals. To elucidate the molecular mechanisms involved in GrnA-regulated liver growth, we performed a cDNA microarray analysis, which showed that GrnA modulated the expression of *met* and other related genes. During embryogenesis, Met and its ligand, the scatter factor/hepatocyte growth factor, play crucial roles in regulating liver development (49), nerve outgrowth (50), and myoblast migration from somites to the limbs (5, 35). In addition, dysregulation of the MET signaling pathway promotes invasive growth and initiates metastasis during tumorigenesis (51, 52). The transcriptional induction of *met* has been determined in human HCC (53, 54), whereas little is known concerning its transcriptional regulation, except for the roles of ETS (55), hypoxia-inducible factor-1a (56), *yb1* (28), and β -catenin (57). The *met* gene is a downstream target of β -catenin (57), and MET is also known to induce β -catenin phosphorylation and accumulation (29). In our model, GrnA-regulated mRNA expression of *yb1*, *ctnnb1*, and other MET related genes were confirmed using quantitative RT-PCR (Fig. 6A). GrnA also regulated *met* and β -cate-

nin expression by Western blotting and WISH analyses (Fig. 8). Furthermore, β -catenin belongs to the Wnt signaling pathway and has been shown to regulate liver growth (58), which suggests that Wnt signaling might also be of relevance and that extensive cellular pathways are affected by the knock-down of GrnA. Hence, it may explain why the *met* mRNA could not fully rescue the *grnA* morphant phenotype (Fig. 7, D and J). In rescue experiments, we found that a co-injection of *met* mRNA with *grnA* MO could restore the impaired liver growth caused by *grnA* MO administration; in contrast, *grnA* mRNA did not rescue the liver size resulting from the knock-down of MET (Fig. 7, F and L). Our results indicate that GrnA might serve as an upstream regulator of MET to regulate embryonic liver growth.

Taken together, we demonstrate that zebrafish *grnA* is required for embryonic hepatic outgrowth, and that GrnA acts, at least partially, through MET signaling to regulate embryonic liver growth. Additionally, we provide a model that could be used to study both genetic and functional factors that are involved in embryonic liver morphogenesis. Because the PGRN receptor and downstream effectors have not yet been identified (59, 60), our work proposes a possible crosstalk be-

tween PGRN and MET signaling and suggests new directions for future studies.

Acknowledgments—We thank Chuang-Yu Lin and Shin-Yi Du for technical support. We also thank Dr. Sheng-Ping L. Hwang for providing the foxA3 construct and the PH3 antibody.

REFERENCES

- Blouin, A., Bolender, R. P., and Weibel, E. R. (1977) *J. Cell Biol.* **72**, 441–455
- Duncan, S. A. (2003) *Mech. Dev.* **120**, 19–33
- Zaret, K. S. (2002) *Nat. Rev. Genet.* **3**, 499–512
- Birchmeier, C., Birchmeier, W., Gherardi, E., and Vande Woude, G. F. (2003) *Nat. Rev. Mol. Cell Biol.* **4**, 915–925
- Bladt, F., Riethmacher, D., Isenmann, S., Aguzzi, A., and Birchmeier, C. (1995) *Nature* **376**, 768–771
- Palmiter, R. D., Norstedt, G., Gelinis, R. E., Hammer, R. E., and Brinster, R. L. (1983) *Science* **222**, 809–814
- Chen, M. H., Li, Y. H., Chang, Y., Hu, S. Y., Gong, H. Y., Lin, G. H., Chen, T. T., and Wu, J. L. (2007) *Gen. Comp. Endocrinol.* **150**, 212–218
- He, Z., and Bateman, A. (2003) *J. Mol. Med.* **81**, 600–612
- Ong, C. H., and Bateman, A. (2003) *Histol. Histopathol.* **18**, 1275–1288
- Cheung, S. T., Wong, S. Y., Leung, K. L., Chen, X., So, S., Ng, I. O., and Fan, S. T. (2004) *Clin. Cancer Res.* **10**, 7629–7636
- Ho, J. C., Ip, Y. C., Cheung, S. T., Lee, Y. T., Chan, K. F., Wong, S. Y., and Fan, S. T. (2008) *Hepatology* **47**, 1524–1532
- Breuhahn, K., Longrich, T., and Schirmacher, P. (2006) *Oncogene* **25**, 3787–3800
- Chu, J., and Sadler, K. C. (2009) *Hepatology* **50**, 1656–1663
- Cadieux, B., Chitramuthu, B. P., Baranowski, D., and Bennett, H. P. (2005) *BMC Genomics* **6**, 156
- Kimmel, C. B., Ballard, W. W., Kimmel, S. R., Ullmann, B., and Schilling, T. F. (1995) *Dev. Dyn.* **203**, 253–310
- Tran, N. L., McDonough, W. S., Savitch, B. A., Sawyer, T. F., Winkles, J. A., and Berens, M. E. (2005) *J. Biol. Chem.* **280**, 3483–3492
- Hu, M. C., Gong, H. Y., Lin, G. H., Hu, S. Y., Chen, M. H., Huang, S. J., Liao, C. F., and Wu, J. L. (2007) *Biochem. Biophys. Res. Commun.* **359**, 778–783
- Nikopoulos, G. N., Adams, T. L., Adams, D., Oxburgh, L., Prudovsky, I., and Verdi, J. M. (2008) *BioTechniques* **44**, 547–549
- Haines, L., Neyt, C., Gautier, P., Keenan, D. G., Bryson-Richardson, R. J., Hollway, G. E., Cole, N. J., and Currie, P. D. (2004) *Development* **131**, 4857–4869
- van de Wetering, M., Cavallo, R., Dooijes, D., van Beest, M., van Es, J., Loureiro, J., Ypma, A., Hursh, D., Jones, T., Bejsovec, A., Peifer, M., Mortin, M., and Clevers, H. (1997) *Cell* **88**, 789–799
- Shepard, J. L., Stern, H. M., Pfaff, K. L., and Amatruda, J. F. (2004) *Methods Cell Biol.* **76**, 109–125
- Alexander, J., Rothenberg, M., Henry, G. L., and Stainier, D. Y. (1999) *Dev. Biol.* **215**, 343–357
- Chou, M. Y., Hsiao, C. D., Chen, S. C., Chen, I. W., Liu, S. T., and Hwang, P. P. (2008) *J. Exp. Biol.* **211**, 3077–3084
- Her, G. M., Yeh, Y. H., and Wu, J. L. (2003) *Dev. Dyn.* **227**, 347–356
- Ober, E. A., Verkade, H., Field, H. A., and Stainier, D. Y. (2006) *Nature* **442**, 688–691
- Miyata, Y., Sagara, Y., Kanda, S., Hayashi, T., and Kanetake, H. (2009) *Hum. Pathol.* **40**, 496–504
- Ren, Y., Chan, H. M., Fan, J., Xie, Y., Chen, Y. X., Li, W., Jiang, G. P., Liu, Q., Meinhardt, A., and Tam, P. K. (2006) *Oncogene* **25**, 3501–3508
- Finkbeiner, M. R., Astanehe, A., To, K., Fotovati, A., Davies, A. H., Zhao, Y., Jiang, H., Stratford, A. L., Shadeo, A., Boccaccio, C., Comoglio, P., Mertens, P. R., Eirew, P., Raouf, A., Eaves, C. J., and Dunn, S. E. (2009) *Oncogene* **28**, 1421–1431
- Danilkovitch-Miagkova, A., Miagkov, A., Skeel, A., Nakaigawa, N., Zbar, B., and Leonard, E. J. (2001) *Mol. Cell. Biol.* **21**, 5857–5868
- Campbell, D. B., Li, C., Sutcliffe, J. S., Persico, A. M., and Levitt, P. (2008) *Autism Res.* **1**, 159–168
- Watanabe, T., Tsuda, M., Makino, Y., Ichihara, S., Sawa, H., Minami, A., Mochizuki, N., Nagashima, K., and Tanaka, S. (2006) *Mol. Cancer Res.* **4**, 499–510
- Grisendi, S., Chambraud, B., Gout, I., Comoglio, P. M., and Crepaldi, T. (2001) *J. Biol. Chem.* **276**, 46632–46638
- Liu, Y., Centracchio, J. N., Lin, L., Sun, A. M., and Dworkin, L. D. (1998) *Exp. Cell Res.* **242**, 174–185
- Nakaigawa, N., Yao, M., Baba, M., Kato, S., Kishida, T., Hattori, K., Nagashima, Y., and Kubota, Y. (2006) *Cancer Res.* **66**, 3699–3705
- Latimer, A. J., and Jessen, J. R. (2008) *Dev. Dyn.* **237**, 3904–3915
- Daniel, R., Daniels, E., He, Z., and Bateman, A. (2003) *Dev. Dyn.* **227**, 593–599
- Bonnard, M., Mirtsos, C., Suzuki, S., Graham, K., Huang, J., Ng, M., Itié, A., Wakeham, A., Shahinian, A., Henzel, W. J., Elia, A. J., Shillinglaw, W., Mak, T. W., Cao, Z., and Yeh, W. C. (2000) *EMBO J.* **19**, 4976–4985
- Rudolph, D., Yeh, W. C., Wakeham, A., Rudolph, B., Nallainathan, D., Potter, J., Elia, A. J., and Mak, T. W. (2000) *Genes Dev.* **14**, 854–862
- Huang, H., Ruan, H., Aw, M. Y., Hussain, A., Guo, L., Gao, C., Qian, F., Leung, T., Song, H., Kimelman, D., Wen, Z., and Peng, J. (2008) *Development* **135**, 3209–3218
- Sadler, K. C., Krahn, K. N., Gaur, N. A., and Ukomadu, C. (2007) *Proc. Natl. Acad. Sci. U.S.A.* **104**, 1570–1575
- He, Z., and Bateman, A. (1999) *Cancer Res.* **59**, 3222–3229
- He, Z., Ismail, A., Kriazhev, L., Sadvakassova, G., and Bateman, A. (2002) *Cancer Res.* **62**, 5590–5596
- Pizarro, G. O., Zhou, X. C., Koch, A., Gharib, M., Raval, S., Bible, K., and Jones, M. B. (2007) *Int. J. Cancer* **120**, 2339–2343
- Kim, W. E., and Serrero, G. (2006) *Clin. Cancer Res.* **12**, 4192–4199
- Tangkeangsirisin, W., Hayashi, J., and Serrero, G. (2004) *Cancer Res.* **64**, 1737–1743
- Kayasuga, Y., Chiba, S., Suzuki, M., Kikusui, T., Matsuwaki, T., Yamanouchi, K., Kotaki, H., Horai, R., Iwakura, Y., and Nishihara, M. (2007) *Behav. Brain Res.* **185**, 110–118
- Yin, F., Banerjee, R., Thomas, B., Zhou, P., Qian, L., Jia, T., Ma, X., Ma, Y., Iadecola, C., Beal, M. F., Nathan, C., and Ding, A. (2010) *J. Exp. Med.* **207**, 117–128
- Yin, F., Dumont, M., Banerjee, R., Ma, Y., Li, H., Lin, M. T., Beal, M. F., Nathan, C., Thomas, B., and Ding, A. (2010) *FASEB J.*, in press
- Schmidt, C., Bladt, F., Goedecke, S., Brinkmann, V., Zschesche, W., Sharpe, M., Gherardi, E., and Birchmeier, C. (1995) *Nature* **373**, 699–702
- Maina, F., Panté, G., Helmbacher, F., Andres, R., Porthin, A., Davies, A. M., Ponzetto, C., and Klein, R. (2001) *Mol. Cell* **7**, 1293–1306
- Suzuki, K., Hayashi, N., Yamada, Y., Yoshihara, H., Miyamoto, Y., Ito, Y., Ito, T., Katayama, K., Sasaki, Y., Ito, A., et al. (1994) *Hepatology* **20**, 1231–1236
- Wang, R., Ferrell, L. D., Faouzi, S., Maher, J. J., and Bishop, J. M. (2001) *J. Cell Biol.* **153**, 1023–1034
- Ueki, T., Fujimoto, J., Suzuki, T., Yamamoto, H., and Okamoto, E. (1997) *Hepatology* **25**, 619–623
- Tavian, D., De Petro, G., Benetti, A., Portolani, N., Giulini, S. M., and Barlati, S. (2000) *Int. J. Cancer* **87**, 644–649
- Gambarotta, G., Boccaccio, C., Giordano, S., Andó, M., Stella, M. C., and Comoglio, P. M. (1996) *Oncogene* **13**, 1911–1917
- Pennacchietti, S., Michieli, P., Galluzzo, M., Mazzone, M., Giordano, S., and Comoglio, P. M. (2003) *Cancer Cell* **3**, 347–361
- Boon, E. M., van der Neut, R., van de Wetering, M., Clevers, H., and Pals, S. T. (2002) *Cancer Res.* **62**, 5126–5128
- Apte, U., Zeng, G., Thompson, M. D., Muller, P., Micsenyi, A., Cieply, B., Kaestner, K. H., and Monga, S. P. (2007) *Am. J. Physiol. Gastrointest. Liver Physiol.* **292**, G1578–G1585
- Lai, A. Z., Abella, J. V., and Park, M. (2009) *Trends Cell Biol.* **19**, 542–551
- Xia, X., and Serrero, G. (1998) *Biochem. Biophys. Res. Commun.* **245**, 539–543